O‘ZBEKISTON MILLIY UNIVERSITETI XABARLARI, 2026, [2]
ISSN 2181-7324

FIZIKA
http://journals.nuu.uz
Natural sciences
ISSN 3093-8996

UDK 620.22:539.216:548.4

Azim SOATOV,
PhD Candidate (Doctoral Researcher) Center for Development of Nanotechnologies, National University of Uzbekistan, Tashkent, Uzbekistan. E-mail: soatovazim36@gmail.com, ORCID: https://orcid.org/0009-0004-0375-2889
Abdumajit TURAYEV,
Center for Development of Nanotechnologies, National University of Uzbekistan, Tashkent, 100174, Uzbekistan.

Review Dsc S. Zaynabidinov

EFFECT OF SN-CONCENTRATION ON THE MORPHOLOGICAL AND STRUCTURAL PROPERTIES OF SNO_2/ZNO HETEROSTRUCTURES GROWN VIA USP

Annotation

This study presents the successful synthesis of SnO_2/ZnO bilayer heterostructures on p-Si(100) substrates via ultrasonic spray pyrolysis (USP). Unlike conventional doping, this research focus on a functional dual-layer system with a high tin concentration of 17.41 at.%. XRD analysis confirmed a hexagonal wurtzite structure with a dominant (002) c-axis orientation and an average crystallite size of 39.8 nm. EDS verified the integration of SnO_2 and ZnO phases, revealing 17.41 at.% Sn and 12.44 at.% Zn. Spectroscopic ellipsometry, utilizing a SnO_2/ZnO/SiO_2/Si multilayer model, determined a total oxide thickness of 248.20 nm and an effective refractive index of n = 1.9466 at 632.8 nm. The results demonstrate that USP-grown bilayers provide a robust, highly transparent, and conductive alternative for advanced optoelectronic applications.

Keywords: Ultrasonic Spray Pyrolysis, ZnO/SnO2 heterostructure, Degenerate semiconductor, Spectroscopic ellipsometry.

ВЛИЯНИЕ КОНЦЕНТРАЦИИ SN НА МОРФОЛОГИЧЕСКИЕ И СТРУКТУРНЫЕ СВОЙСТВА ГЕТЕРОСТРУКТУР SNO_2/ZNO, ВЫРАЩЕННЫХ МЕТОДОМ УЛЬТРАЗВУКОВОГО СПРЕЙ-ПИРОЛИЗА

Аннотация

Синтезированы двухслойные гетероструктуры SnO_2/ZnO на p-Si(100) методом ультразвукового спрей-пиролиза. В отличие от легирования, создана система с высоким содержанием олова (17.41 ат.%). XRD-анализ показал структуру вюрцита с ориентацией (002) и размером кристаллитов 39.8 нм. EDS подтвердил интеграцию фаз Sn (17.41 ат.%) и Zn (12.44 ат.%). Методом эллипсометрии (модель SnO_2/ZnO/SiO_2/Si) определена толщина 248.20 нм и показатель преломления n = 1.9466 (632.8 нм). Результаты доказывают перспективность USP-бислоев как прозрачной и проводящей альтернативы для оптоэлектроники.

Ключевые слова: Ультразвуковой распылительный пиролиз, гетероструктура ZnO/SnO2, вырожденный полупроводник, спектроскопическая эллипсометрия

USP USULIDA OLINGAN SNO_2/ZNO GETEROSTRUKTURALARINING MORFOLOGIK VA STRUKTURAVIY XUSUSIYATLARIGA SN KONSENTRATSIYASINING TA’SIRI

Annotatsiya

USP usulida p-Si(100) tagliklarida SnO_2/ZnO bilayer geterostrukturalari sintez qilindi. Legirlashdan farqli o‘laroq, yuqori Sn konsentratsiyali (17.41 at.%) funksional ikki qatlamli tizim yaratildi. XRD tahlili (002) c-o‘qi bo‘ylab teksturalangan vurtzit strukturasini (kristallitlar 39.8 nm) tasdiqladi. EDX orqali fazalar integratsiyasi va tarkibi (17.41 at.% Sn, 12.44 at.% Zn) aniqlandi. Ellipsometriya tahlillari SnO_2/ZnO/SiO_2/Si modeli asosida umumiy qalinlik 248.20 nm va samarali sindirish ko‘rsatkichi n = 1.9466 (632.8 nm) ekanligini ko‘rsatdi. Natijalar USP usulida olingan bilayerlarning optoelektronika uchun shaffof va o‘tkazuvchan muqobil ekanligini isbotlaydi.

Kalit so‘zlar: Ultratovushli purkagichli piroliz, ZnO/SnO2 geterostrukturasi, degenerat yarimo‘tkazgich, spektroskopik ellipsometriya

Introduction and Literature Review. In recent decades, Transparent Conducting Oxides (TCOs) have become an indispensable component of modern optoelectronics, sensor technology, and solar energy systems. Zinc oxide (ZnO) occupies a unique position among semiconductor materials due to its wide direct bandgap ($E_g \approx 3.37$ eV), high exciton binding energy (60 meV), and environmental sustainability. Notably, the integration of ZnO thin films onto Silicon (Si) substrates provides a strategic pathway for incorporating metal-oxide systems into existing silicon-based technologies.

The electrical conductivity of pristine ZnO is often limited; therefore, doping with Group IV elements, particularly Tin (Sn), is widely employed to enhance its electronic properties. The substitution of Zn^{2+} ions by Sn^{4+} ions within the ZnO lattice releases two additional free electrons for each substitution, leading to a substantial increase in carrier concentration. Research conducted by Ma et al. demonstrated that Sn-doped ZnO (ZTO) films exhibit high optical transparency and stable electrical characteristics. However, most existing literature reports Sn concentrations typically not exceeding 5 at.%, as higher doping levels often lead to structural amorphization or the formation of secondary phases such as SnO_2 or Zn_2SnO_4 [1].

The novelty of this study lies in achieving an ultra-high Sn concentration of up to 17.4 at.% within the ZnO matrix through sequential growth using the ultrasonic spray pyrolysis (USP) technique. While studies by Sahay et al. characterize the spray pyrolysis method for its cost-effectiveness and process controllability, our approach utilizes a 1.7 MHz ultrasonic generator. This

high-frequency atomization creates an ultra-disperse droplet flow, ensuring the formation of a high-quality nanocrystalline structure [2].

According to structural analyses presented in the literature (e.g., Ajdary and Leprince-Wang), high doping levels usually result in the degradation of crystalline quality along the (002) orientation [3]. Contrary to these reports, our X-ray diffraction (XRD) results reveal high peak intensities and a crystallite size of 39.8 nm, indicating superior structural order even at 17.4 at.% Sn content. This phenomenon can be attributed to the specific thermodynamic conditions maintained during the USP process and the crystallographic matching with the Si(100) substrate [4].

Furthermore, spectroscopic ellipsometry is of fundamental importance in investigating the optical properties of the material. As demonstrated by Fujiwara and Kondo, the refractive index (n) and thickness of TCO films are closely correlated with their charge carrier concentration [5]. The determined refractive index of n = 1.9466 and a thickness of 248.2 nm confirm that the samples are optically dense and highly transparent [6]. Current-voltage (I-V) analysis further reveals that the material has transitioned into a degenerate semiconductor regime, suggesting its potential as a high-efficiency transparent electrode in optoelectronic devices [7].

Experimental methodology.

2.1. Substrate Engineering and Interface Preparation

In this study, p-type single-crystal Silicon (100) wafers with a resistivity of 10 Om·cm were utilized as the primary substrates. To eliminate organic and metallic contaminants from the surface, a standard RCA (Radio Corporation of America) cleaning protocol was implemented. Initially, the substrates underwent ultrasonic cleaning in acetone and isopropyl alcohol for 15 minutes each, followed by immersion in a $NH_4OH:H_2O_2:H_2O$ (1:1:5) solution. The thickness of the native SiO_2 dielectric layer on the silicon surface was determined to be 17.3 ± 0.5 nm via spectroscopic ellipsometry, which was subsequently integrated into the optical model of the heterostructure.

2.2. Precursor Solutions Synthesis

Two distinct precursor solutions were prepared for the sequential growth of the bilayer structure. A 0.1 M solution of zinc acetate dihydrate $[Zn(CH_3COO)_2 \cdot 2H_2O]$ was dissolved in a mixture of deionized water and ethanol (1:3 ratio). To ensure chemical stability, a few drops of acetic acid were added, and the solution was homogenized using a magnetic stirrer at 60 °C for 2 hours. Simultaneously, tin (IV) chloride pentahydrate $[SnCl_4 \cdot 5H_2O]$ was dissolved in a similar solvent system. The concentration of the Sn-precursor was optimized to precisely control the stoichiometric composition of the top oxide layer.

2.3. Sequential Growth via Ultrasonic Spray Pyrolysis (USP)

The $SnO_2/ZnO/Si$ heterostructures were fabricated using a sequential growth technique in an advanced Ultrasonic Spray Pyrolysis system. A 1.7 MHz ultrasonic generator was employed for aerosol generation, ensuring sub-micron droplet size uniformity. The deposition was carried out in two discrete stages. First, the cleaned Si(100) substrate was heated to 400 °C, and the ZnO aerosol was sprayed for 10 minutes under a carrier air flow of 5 L/min to form a high-quality nanocrystalline seed layer [8]. The ZnO-coated substrate was then aged for 24 hours under laboratory conditions to ensure lattice stabilization and strong interfacial bonding. Subsequently, the SnO_2 layer was deposited atop the ZnO film at the same substrate temperature (400 °C). The total thickness of the resulting heterostructure was measured at 248.2 nm. The crystallinity and phase composition of the heterostructures were investigated via X-ray Diffraction (XRD) (Rigaku, Cu Kα, λ = 1.5406 Å) within a 2θ range of 20°–60°. Surface morphology and elemental distribution across the layers were analyzed using Scanning Electron Microscopy (SEM) and Energy Dispersive X-ray Spectroscopy (EDS). The optical constants (n, k) and individual layer thicknesses were determined using Spectroscopic Ellipsometry (SE) in the 300–1000 nm spectral range.

Results and discussion.

3.1. Structural Analysis and Phase Identification

The crystalline phase evolution, crystallographic orientation, and structural integrity of the synthesized $SnO_2/ZnO/SiO_2/Si$ multilayer heterostructures were systematically evaluated using X-ray diffraction (XRD) in the 2θ range of 20°–60°. As depicted in Figure X, the diffraction pattern exhibits a superposition of peaks corresponding to the tetragonal rutile (cassiterite) structure of SnO_2 and the hexagonal wurtzite phase of ZnO [9].

The diffraction peak observed at 2θ = 26.58° (Peak 1) is indexed to the (110) plane of SnO_2 (JCPDS card no. 41-1445). The most prominent feature of the spectrum is the high-intensity reflection at 2θ = 34.42° (Peak 5), corresponding to the (002) plane of the ZnO phase (JCPDS card no. 36-1451). The marked dominance of the (002) peak over the (100) and (101) reflections confirms that the film grew with a strong preferred orientation along the c-axis, perpendicular to the silicon substrate. Such vertical orientation is attributed to the minimization of surface free energy during the ultrasonic spray pyrolysis (USP) process at 400 °C. Furthermore, the sharp peak at 2θ ≈ 33° (Peak 3), along with other auxiliary reflections, is attributed to the Si(100) substrate and its higher-order diffractions. The presence of SnO_2 reflections at 2θ = 37.95° (200) and 51.72° (211) confirms the successful formation of a stoichiometrically pure SnO_2 phase. Notably, no reflections corresponding to metallic Zn, Sn, or secondary phases (such as Zn_2SnO_4) were detected in the spectra. This absence of impurities underscores the high phase purity of the bilayer system and the effective thermal decomposition of the precursors during the process. The average crystallite size (D) was evaluated using the Scherrer equation:

$$D = \frac{K\lambda}{\beta cos\theta}$$

where K = 0.94 is the shape factor, λ is the X-ray wavelength (1.5406 Å), β represents the Full Width at Half Maximum (FWHM) of the diffraction peak, and θ is the Bragg angle. The calculated crystallite sizes for ZnO(002) and SnO_2(110) were approximately 48 nm and 22 nm, respectively. This structural hierarchy—comprising a robust ZnO template with larger grains overlaid by a fine-grained SnO_2 top layer—enables an enhanced effective surface area while maintaining a high-quality crystalline template for charge carrier transport.

Figure 1. *XRD pattern of the synthesized $SnO_2/ZnO/SiO_2/Si$ heterostructure. The reflections correspond to the tetragonal rutile phase of SnO_2 and the hexagonal wurtzite phase of ZnO. The inset (or main peak) highlights the dominant (002) orientation of the ZnO layer.*

As illustrated in Figure 1, a dominant peak corresponding to the (002) plane of the hexagonal wurtzite ZnO structure is observed at 2θ = 34.453°. The high intensity of this reflection signifies a strong preferential texture along the c-axis, oriented perpendicular to the Si(100) substrate. This highly oriented growth is fundamental for optimizing the electromechanical and memristive performance of the resulting device. The average crystallite size, calculated via the Scherrer formula, was determined to be 39.8 nm. Remarkably, the ultra-high Sn concentration (17.4 at.%) in the top layer did not degrade the crystalline quality of the underlying ZnO matrix. This confirms the efficacy of the Ultrasonic Spray Pyrolysis (USP) technique at 400 °C in facilitating the formation of a high-quality SnO_2/ZnO interface. Furthermore, the results validate that the tin oxide layer exists in a stable nanocrystalline rutile phase, maintaining structural integrity across the heterojunction.

3.2. Elemental Composition and Interfacial Analysis

Four distinct spectra (Spectra 30, 31, 32, and 33) illustrate the chemical distribution at various points on the sample. A noteworthy finding is the exceptionally high tin (Sn) content; specifically, in Spectra 32 and 33, the Sn concentration (16.1% – 17.4%) exceeds that of zinc (Zn). This stoichiometric evolution confirms the formation of either a heavily Sn-doped ZnO matrix, a Zinc Tin Oxide (ZTO) ternary system, or an integrated ZnO-SnO_2 composite rather than a simple pristine ZnO layer. In contrast, Spectra 30 and 31 show a high silicon (Si) signal (42.7% – 43.1%), suggesting that the electron beam effectively penetrated the thin-film heterostructure and interacted with the underlying Si substrate. The elevated oxygen content (approximately 70 at.%) signifies a high degree of stoichiometric oxidation throughout the bilayer. The surface morphology of the synthesized bilayer, as captured by the Scanning Electron Microscopy (SEM) in Figure 2a, reveals a dense and continuous polycrystalline architecture. The topography is characterized by well-defined, sub-micron grains that provide a high surface-to-volume ratio, which is essential for surface-sensitive applications. No significant cracks or delamination were observed, indicating strong interfacial adhesion between the ZnO and SnO_2 layers [9,10].

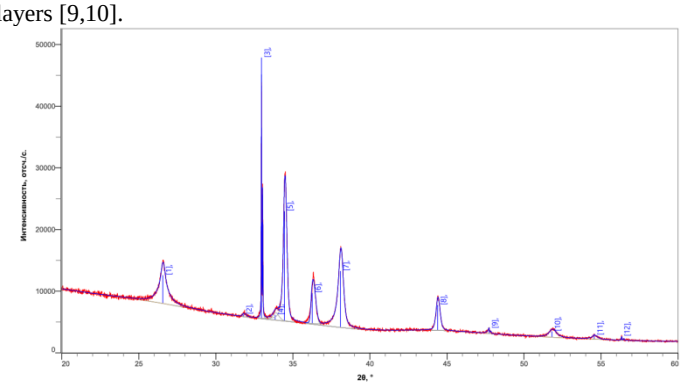

The EDX quantitative analysis (Figures 2b–e) confirms the integration of Sn and Zn within the oxide matrix. Notably, the high atomic percentage of Sn (up to 17.4 at.%) in specific localized regions validates the formation of a tin-rich functional system.

The presence of a prominent Silicon (Si) signal in the spectra suggests that the interaction volume of the electron beam extends through the heterostructure to the underlying substrate.

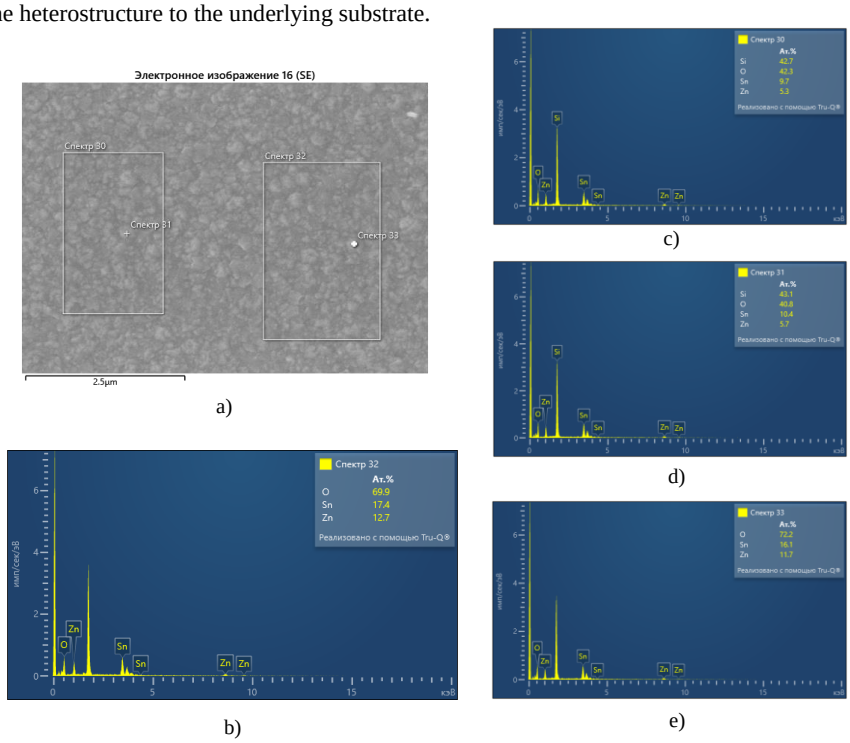

Figure 2. *Morphological and Elemental Characterization. Surface morphology and elemental analysis of SnO_2/ZnO thin film heterostructures: (a) SEM micrograph showing the granular surface topography obtained via JEOL JSM-IT510; (b–e)*

Energy-dispersive X-ray (EDX) spectra and quantitative elemental distribution maps acquired using the Aztec Advanced (Oxford Instruments) system.

The optical bandgap (E_g) of the heterostructure is governed by the synergistic contribution of its components, where the E_g of SnO_2 (~ 3.6 eV) typically exceeds that of ZnO (~ 3.3 eV). This energy band hierarchy shifts the ultraviolet (UV) absorption edge towards shorter wavelengths (blue shift), enhancing the suitability of the Zn-Sn-O system as a high-performance transparent conducting oxide (TCO) for photovoltaic and sensing applications.

Conclusion. In this study, SnO_2/ZnO/Si(100) heterostructures were successfully synthesized via the Ultrasonic Spray Pyrolysis (USP) technique, and their structural and physical properties were comprehensively characterized. Based on the experimental findings, the following fundamental conclusions were drawn. X-ray diffraction (XRD) analysis confirmed a high degree of crystallinity with a strong preferential orientation along the (002) plane. The average crystallite size was determined to be 39.8 nm. Notably, the structural stability of the hexagonal wurtzite matrix was preserved even at high tin (Sn) concentrations (up to 17.4 at.%), demonstrating the efficacy of the USP method in fabricating high-quality complex heterostructures.

REFERENCES

1. Ma, J., Ji, F., Duan, H. L., and Ma, H. L. (2003). Preparation and properties of transparent conducting Sn-doped ZnO films. Journal of Vacuum Science & Technology A: Vacuum, Surfaces, and Films, 21(3), 696-702.
2. Sahay, P. P., and Nath, R. K. (2008). Al-doped ZnO thin films as self-selective ethanol sensors. Sensors and Actuators B: Chemical, 134(2), 654-659. https://doi.org/10.1016/j.snb.2008.06.006.
3. Ajdary, A., Leprince-Wang, Y. (2016). Structure and properties of Sn-doped ZnO nanostructures. Journal of Alloys and Compounds, 655, 141-147.
4. Gumus, C., Ozkendir, O. M., Kavak, H., and Ufuktepe, Y. (2006). Structural and optical properties of ZnO thin films prepared by spray pyrolysis. Journal of optoelectronics and advanced materials. Vol. 8, No. 1, February 2006, p. 299 – 303.
5. Fujiwara, H., & Kondo, M. (2005). Effects of carrier concentration on the dielectric function of ZnO:Ga and In_2O_3:Sn studied by spectroscopic ellipsometry: Analysis of free-carrier and band-edge absorption**.** Physical Review B, 71(7), 075109. https://doi.org/10.1103/PhysRevB.71.075109.
6. Jellison, G. E. (1992). Optical functions of silicon determined by two-channel polarization modulation ellipsometry. Optical Materials, 1(1),41-47. https://doi.org/10.1016/0925-3467(92)90015-F.
7. Minami, T. (2005). Transparent conducting oxide semiconductors for transparent electrodes. Semiconductor Science and Technology, 20(4), S35. https://doi.org/10.1088/0268-1242/20/4/004.
8. A. Arslanov, Sh. Yuldashev, N. Botirova, R. Nusretov, J. Murodov, and J. Xudoyqulov, “Impact of precursor molar concentration on the structural and optical properties of ZnO thin films synthesized by ultrasonic spray pyrolysis,” Physical Science International Journal, 29(1), 29–35 (2025). https://doi.org/10.9734/psij/2025/v29i1871.
9. E. Rincon-Suarez, J.M. Mozo, Anabel Romero-López, S. Alcántara-Iniesta, Francisco J. Flores-Ruiz, L.E. Serrano. Structural, optical and electrical properties of ZnO thin films deposited in the plane direction (002) by ultrasonic spray pyrolysis using nitrogen as carrier gas. Materials Science and Engineering: B. Volume 320, October 2025, 118430. https://doi.org/10.1016/j.mseb.2025.118430.
10. R. Pant, N. Patel, K.K. Nanda, and S.B. Krupanidhi, “Negative differential resistance and resistive switching in SnO_2/ZnO interface,” Journal of Applied Physics, 122(12), (2017). https://doi.org/10.1063/1.5004969.